

## Class III $\beta$ -Tubulin and $\gamma$ -Tubulin are Co-expressed and Form Complexes in Human Glioblastoma Cells

Christos D. Katsetos · Eduarda Dráberová · Barbora Šmejkalová · Goutham Reddy · Louise Bertrand · Jean-Pierre de Chadarévian · Agustin Legido · Jonathan Nissanov · Peter W. Baas · Pavel Dráber

Accepted: 22 February 2007 / Published online: 4 April 2007  
© Springer Science+Business Media, LLC 2007

**Abstract** We have previously shown that the neuronal-associated class III  $\beta$ -tubulin isotype and the centrosome-associated  $\gamma$ -tubulin are aberrantly expressed in astrocytic gliomas (Cell Motil Cytoskeleton 2003, 55:77-96; J Neuro-pathol Exp Neurol 2006, 65:455–467). Here we determined the expression, distribution and interaction of  $\beta$ III-tubulin and  $\gamma$ -tubulin in diffuse-type astrocytic gliomas (grades II-IV) ( $n = 17$ ) and the human glioblastoma cell line T98G. By immunohistochemistry and immunofluorescence microscopy,  $\beta$ III-tubulin and  $\gamma$ -tubulin were co-distributed in anaplastic astrocytomas and glioblastomas and to a lesser extent, in low-grade diffuse astrocytomas ( $P < 0.05$ ). In

T98G glioblastoma cells  $\beta$ III-tubulin was associated with microtubules whereas  $\gamma$ -tubulin exhibited striking diffuse cytoplasmic staining in addition to its expectant centrosome-associated pericentriolar distribution. Treatment with different anti-microtubule drugs revealed that  $\beta$ III-tubulin was not associated with insoluble  $\gamma$ -tubulin aggregates. On the other hand, immunoprecipitation experiments unveiled that both tubulins formed complexes in soluble cytoplasmic pools, where substantial amounts of these proteins were located. We suggest that aberrant expression and interactions of  $\beta$ III-tubulin and  $\gamma$ -tubulin may be linked to malignant changes in glial cells.

**Keywords**  $\gamma$ -Tubulin · Class III  $\beta$ -tubulin · Centrosome amplification · Astrocytoma · Glioma · Glioblastoma

C.D. Katsetos and E. Dráberová contributed equally to this work.

C. D. Katsetos · G. Reddy · A. Legido  
Department of Pediatrics, Drexel University College of Medicine and St. Christopher's Hospital for Children, Philadelphia, PA, USA

C. D. Katsetos · J.-P. de Chadarévian  
Department of Pathology and Laboratory Medicine, Drexel University College of Medicine and St. Christopher's Hospital for Children, Philadelphia, PA, USA

E. Dráberová · B. Šmejkalová · P. Dráber  
Laboratory of the Biology of Cytoskeleton, Institute of Molecular Genetics, Academy of Sciences of the Czech Republic, Prague, Czech Republic

L. Bertrand · J. Nissanov · P. W. Baas  
Department of Neurobiology and Anatomy, Drexel University College of Medicine, Philadelphia, PA, USA

C. D. Katsetos (✉)  
Section of Neurology, St. Christopher's Hospital for Children, Erie Avenue at Front Street, Philadelphia, PA 19134, USA  
e-mail: Christos.Katsetos@DrexelMed.edu

### Abbreviations

ANOVA	Analysis of variance
Cy3	Indocarbocyanate
DAPI	4'-6-Diamidino-2-phenylindole
DMEM	Dulbecco's modified Eagle medium
EDTA	Ethylene diamine tetraacetic acid
EGTA	Ethylene glycol tetraacetic acid
FITC	Fluorescein isothiocyanate
GCP	$\gamma$ -Tubulin complex protein
$\gamma$ -TuRC	Large $\gamma$ -tubulin-ring complex
$\gamma$ -TuSC	$\gamma$ -Tubulin-small complex
LI	Labeling index
MES	2-(N-morpholine)-ethane sulphonic acid
MLI	Mean labeling index
MSB	Microtubule-stabilizing buffer
MTOC	Microtubule organizing center
TBST	Tris-Buffered Saline Tween-20

## Introduction

The class III  $\beta$ -tubulin ( $\beta$ III-tubulin) is widely accepted as a marker of neuronal differentiation in developmental neurobiology (reviewed in [1, 2]). Previous studies conducted by members of our laboratories have shown that  $\beta$ III-tubulin expression in human neuronal/neuroblastic tumors of the central and peripheral nervous systems is differentiation-dependent and associated with neuritogenesis in maturing tumor phenotypes (reviewed in [1–4]). By the same token, we have previously shown that  $\beta$ III-tubulin is also aberrantly expressed in various histological types of non-neuronal tumors, including gliomas [1, 2]. Among glial tumors,  $\beta$ III-tubulin is expressed in diffuse astrocytic gliomas and glioblastomas [5, 6], oligodendrogliomas [7], pleomorphic xanthoastrocytomas [6, 8] and related developmental tumors with ambiguous glioneuronal differentiation (reviewed in [2]). In the context of diffuse astrocytomas and oligodendrogliomas  $\beta$ III-tubulin expression relates to an ascending scale of histological malignancy [1, 2, 5, 7].

$\gamma$ -Tubulin is the major cytoskeletal constituent of the pericentriolar matrix of centrosomes, the cell's microtubule organizing centers (MTOCs) where  $\gamma$ -tubulin ring complexes serve as a template for microtubule nucleation [9–11] and play a role in the regulation of cell cycle progression [12].  $\gamma$ -Tubulin interacts with  $\alpha/\beta$ -tubulin dimers and may subserve diverse, albeit hitherto poorly understood, cellular functions [9, 13–16].

We have recently demonstrated that overexpression and altered cellular distribution of  $\gamma$ -tubulin could lead to centrosome amplification as one of the putative mechanism(s) of tumor progression in astrocytomas [17]. Since the recruitment of  $\gamma$ -tubulin ring complexes is a prerequisite for increased microtubule-nucleating activity, we have reasoned that altered profiles of tubulin expression may potentially cause abnormal/ectopic microtubule nucleation in neoplastic glial phenotypes [17].

In this light, we have hypothesized that the aberrant expression of  $\beta$ III-tubulin in astrocytic gliomas may be connected to increased expression of  $\gamma$ -tubulin in the context of centrosome dysfunction and/or amplification [1, 17]. Given that both  $\beta$ III-tubulin and  $\gamma$ -tubulin are known to exhibit altered patterns of expression in neoplastic glial phenotypes as compared to normal astroglial cells [5, 17], we aimed to elucidate the cellular distribution, spatial relationship and interaction of  $\beta$ III-tubulin and  $\gamma$ -tubulin in human primary astrocytic gliomas and the glioblastoma cell line T98G.

## Experimental procedure

### Tissue samples

We evaluated 17 surgically resected samples of diffuse astrocytic gliomas from adults ( $n = 12$ ) and children

( $n = 5$ ) representative of the World Health Organization (WHO) histological grades II–IV. The tumor specimens from adult patients included low-grade diffuse astrocytomas/grade II ( $n = 5$ ), anaplastic astrocytomas/grade III ( $n = 2$ ) and glioblastomas multiforme/grade IV ( $n = 5$ ). The five pediatric glioma specimens included examples of anaplastic glioma of the thalamus and brainstem (grade III) ( $n = 2$ ), and diffuse gliomas (grade II) of the cerebral hemispheric white matter ( $n = 1$ ) and brainstem ( $n = 2$ ). Microtome sections from archived formalin-fixed, paraffin-embedded tissue blocks were cut at 5  $\mu$ m in thickness and stained with hematoxylin and eosin for morphological evaluation. Adjacent, serially cut, and sequentially numbered sections were processed for immunohistochemistry and immunofluorescence microscopy. Control tissues included surgical and autopsy tissue samples from cases devoid of tumor ( $n = 5$ ). All tumor specimens utilized in this study were also used in previous studies [5, 17]. The use of pathological specimens in the present study was subject to approval by Institutional Review Board (IRB) Exempt Review. No patient identifiers were used.

### Glioblastoma cell line

A well-established, p53 mutant, human glioblastoma cell line, T98G [18, 19] was obtained from the American Type Culture Collection (ATCC) (Manassas, Virginia, USA). The cell line was maintained in 10% FBS in Dulbecco's modified Eagle medium (DMEM) at 37°C. To some of the T98G cell cultures nocodazole (Sigma), taxol (National Cancer Institute, Bethesda, Maryland, USA) and vinblastine (Gedeon Richter, Budapest Hungary) were added at 10  $\mu$ M for 18 h. Also, 3T3 cells (mouse embryonic fibroblasts) grown in Eagle's minimal essential medium supplemented with 10% FBS were used as control.

### Antibodies

For the detection of class III  $\beta$ -tubulin two mouse monoclonal antibodies, TuJ1 (IgG2a) and TU-20 (IgG1) directed against epitopes on the C-terminal end of the neuron-specific  $\beta$ III-tubulin were used. The characterization, purification and production of TuJ1 has been described elsewhere [20–22]. The predominantly neuronal cell type specificity of monoclonal antibody TuJ1 in developing and mature, non-neoplastic human tissues has been elucidated in previous studies [1, 2, 23, 24]. TU-20 was prepared against a conserved synthetic peptide from the C-terminus of the human class III  $\beta$ -tubulin isotype [3]. Similarly, the specificity of TU-20 antibody has been demonstrated previously [3, 25, 26]. In addition, an affinity purified rabbit antibody against the CMYEDDDDEESEAQGPK peptide

identical to the  $\beta$ III carboxyl terminal, isotype-defining domain detected by monoclonal antibody TuJ1, was used [27].

For the detection of  $\gamma$ -tubulin, four monoclonal anti-peptide antibodies recognizing epitopes in C-terminal or N-terminal domains of the  $\gamma$ -tubulin molecule were used. These included GTU-88 (IgG1) generated against the EEFATEGTDRKDVFFY peptide corresponding to the human sequence 38–53 in the N-terminal region of  $\gamma$ -tubulin sequence (Sigma Aldrich cat. no. T6557) and antibodies TU-30 (IgG2b), TU-31 (IgG2b) and TU-32 (IgG1) generated against EYHAATRPDYISWGTQ peptide corresponding to the human sequence 434–449 in the C-terminal region of  $\gamma$ -tubulin [28]. Specificity of these antibodies for  $\gamma$ -tubulin was verified in various cell types [24, 29, 30] was extensively characterized. Mouse monoclonal antibody NF-09 (IgG2a) against neurofilament protein NF-M [31] and rabbit antibody against non-muscle myosin (Biomedical Technologies Inc., Stoughton, Massachusetts, USA) were used as negative controls in immunoprecipitation experiments.

Indocarbocyanate (Cy3)-conjugated anti-mouse, and FITC-conjugated anti-rabbit antibodies for multiple staining were from Jackson ImmunoResearch Laboratories (West Grove, Pennsylvania, USA). FITC-conjugated anti-mouse antibody was also bought from Vector Laboratories (Burlingame, California, USA). Texas Red-conjugated anti-rabbit antibody was purchased from Vector Laboratories. Anti-mouse and anti-rabbit antibodies conjugated with horseradish peroxidase were purchased from Promega Biotec (Madison, Wisconsin, USA).

#### Immunohistochemistry on primary tumors

Prior to immunohistochemistry, 5  $\mu$ m thick histological sections from paraffin-embedded tissue blocks were subjected to microwave antigen unmasking in  $\text{Na}^+$  EDTA buffer at pH 8.0. Immunohistochemistry was performed according to the avidin biotin complex (ABC) peroxidase method using the Mouse IgG ABC Elite® detection kit (Vector Labs, Burlingame, California, USA) as previously described [5]. Anti- $\beta$ III-tubulin (TuJ1) and anti- $\gamma$ -tubulin (GTU-88) monoclonal antibodies were diluted 1:500 and 1:300 respectively. Negative controls included omission of primary antibody and substitution with nonspecific mouse IgG1 and IgG2b, which were used as immunoglobulin class-specific controls (corresponding to the immunoglobulin subclasses of the primary antibodies employed in this study) (Becton Dickinson, Franklin Lakes, New Jersey, USA). Experiments using non-conjugated isotype matched control monoclonal antibodies did not show any non-specific binding of the secondary rabbit anti-mouse IgG1 and IgG2b antibodies.

Histologic preparations were evaluated independently by a neuropathologist (C.D.K.) and a pediatric pathologist (J-P.D.) who were blinded as to the pathological diagnosis and tumor grade designation originally rendered for each specimen. All 17 surgically resected tumor specimens were included in previous studies on  $\beta$ III-tubulin and  $\gamma$ -tubulin detection in astrocytic gliomas [5, 17].

The minimal criterion for the identification of a  $\gamma$ -tubulin -positive cell in the context of an abnormal staining pattern associated with putative centrosome amplification, was the detection of 3 or more punctate, dot-like immunoreactive signals, or diffuse staining, in the cytoplasm of a single tumor cell as previously described [17].

Manual cell counting of labeled tumor cells was performed by 2 observers independently (C.D.K., G.R.). Cell counting and statistical analysis were carried out only in the adult group of astrocytic gliomas ( $n = 12$ ). Between 456 and 872 tumor cells were evaluated per case, in 20 non-overlapping high-power (40 $\times$ ) fields and a labeling index was determined for each case. Labeling index (LI) was expressed as the percentage (%) of either  $\beta$ III-tubulin or  $\gamma$ -tubulin labeled cells out of the total number of tumor cells counted in each case and for each antibody. Interobserver agreement for the evaluation of immunohistochemical staining was within 15% ( $k = 0.82$ ) [5]. The median labeling index (MLI) and the interquartile range (IQR) - delimited by the 25th and 75th percentiles- were determined for the set of cases in each histological grade using one-way ANOVA (Jandel software, Sigmastat). The statistical significance of differences in labeling indices between WHO histological grades were examined with non-parametric statistical techniques using Kruskal-Wallis analysis of variance tests. A p value of less than 0.05 was considered as statistically significant. Because of the small number of pediatric gliomas ( $P = 5$ ) included in this study, only qualitative assessment was performed in these cases.

#### Immunofluorescence on primary tumors

Sections from formalin-fixed, paraffin-embedded tumor tissues obtained after surgical resection were utilized for immunofluorescence microscopy as described previously [17]. For double-labeling immunofluorescence studies on deparaffinized archival histological sections, monoclonal antibody GTU-88 against  $\gamma$ -tubulin, and the polyclonal anti- $\beta$ III-tubulin antibodies were diluted 1:500. FITC-conjugated anti-mouse and Texas Red-conjugated anti-rabbit antibodies were diluted 1:200. 4,6-Diamidino-2-phenylindole (DAPI) was used to label cell nuclei. Slides were cover-slipped using an aqueous based mounting medium (Vector Laboratories).

Immunostained sections were evaluated with a Leica TCS SP2 AOBS (Acousto-Optical Beam Splitter) laser

confocal system equipped with a Leica DMRE fluorescence microscope. This system is outfitted with an SP prism spectrophotometer and four sets of movable slit in front of the detection photomultiplier (PMT) used for detection of fluorescence emission and minimization of crosstalk. For balanced excitation of the fluorochromes, the lasers are combined with acoustico-optical tunable filter (AOTF) system, which enables to adjust the individual intensity of the three laser lines (Argon - 488 nm, Green neon - 543 nm, and helium neon - 633 nm) independently. A diode (UV laser - 405 nm) is also part of this system.

DAPI was excited by 405 nm beam using a neutral density filter of 50 and was detected through a spectral of 410–482 nm (emission peak of 456 nm); FITC was excited by 488 nm laser beam and was detected through a spectral range of 500–538 nm (emission peak of 520 nm); Texas Red was excited by the 543 nm beam and was detected through a spectral range of 589–713 nm (emission peak of 620 nm).

#### Immunofluorescence on T98G glioblastoma cell line

Immunofluorescence microscopy on fixed cells was performed as described previously [32]. Cells grown on coverslips, were rinsed briefly with MSB buffer supplemented with 4% polyethylene glycol 6000, extracted for 2 min with 0.2% Triton X-100 in MSB and fixed for 20 min in 3% formaldehyde in MSB. When  $\gamma$ -tubulin was detected, coverslips were postfixed for 10 min in methanol at  $-20^{\circ}\text{C}$ .

Monoclonal anti- $\beta$ III-tubulin antibody TuJ1 was diluted 1:250. Antibody TU-20 was used as undiluted supernatant. The polyclonal antibody against  $\beta$ III-tubulin was diluted 1:500. Monoclonal antibodies against  $\gamma$ -tubulin TU-30 and TU-31 were used as undiluted supernatants. Cy3-conjugated anti-mouse antibody was diluted 1:50. FITC-conjugated anti-rabbit antibody was diluted 1:100.

For double-label staining of  $\beta$ III-tubulin and  $\gamma$ -tubulin, the coverslips were incubated simultaneously with anti- $\gamma$ -tubulin antibody TU-30 and polyclonal anti- $\beta$ III-tubulin antibody. After washing, the coverslips were incubated simultaneously with the secondary fluorochrome-conjugated antibodies. DAPI was used to label cell nuclei. The preparations were mounted in MOWIOL 4-88 (Calbiochem) and examined with Olympus A70 Provis microscope. As negative controls served conjugates alone that did not give any detectable staining.

#### Preparation of cell extracts

For preparation of soluble and detergent-resistant fractions at  $37^{\circ}\text{C}$ , cells on 6-cm Petri dishes were either directly used for the assay or they were before assay

preincubated 6 h with  $0.5\ \mu\text{g}$  nocodazole/ml to disrupt microtubule arrays. Attached cells were rinsed twice in microtubule-stabilizing (MSB) buffer (100 mM MES adjusted to pH 6.9 with KOH, 2 mM EGTA, 2 mM  $\text{MgCl}_2$ ) or in MSB buffer containing nocodazole (MSB/nocodazole), and then extracted with 0.5 ml of MSB buffer ( $37^{\circ}\text{C}$ ) or MSB/nocodazole supplemented with, protease inhibitor cocktail (“Complete EDTA-free” tablets) (Roche Molecular Biochemicals, Mannheim, Germany), phosphatase inhibitors (1 mM  $\text{Na}_3\text{VO}_4$ , 1 mM NaF) and 0.2% (v/v) Triton X-100. After 1 min incubation at  $37^{\circ}\text{C}$ , the extract was gently removed, spun down at  $5\ 000\ g$  for 1 min at  $25^{\circ}\text{C}$ , and one-fourth volume of  $4\times$  SDS/PAGE-sample buffer was added to the supernatant. The cytoskeletons remaining on the plate were gently rinsed twice with warm MSB buffer containing inhibitors and solubilized with 0.625 ml of sample buffer, prepared by mixing  $2\times$  SDS/PAGE-sample buffer with  $2\times$  extraction buffer (1:1). Pelleted material obtained after spinning down the extract was combined with the cytoskeletal fraction. Samples were boiled for 5 min.

When preparing the extract for immunoprecipitation, cells were rinsed twice in cold MSB and extracted 2 min at  $4^{\circ}\text{C}$  with MSB buffer (0.5 ml/dish) supplemented with protease and phosphatase inhibitors and 0.2% Triton X-100. The suspension was then spun down ( $20,000g$ , 15 min,  $4^{\circ}\text{C}$ ), and supernatant collected.

#### Immunoprecipitation

Immunoprecipitation was performed as described previously [32] using TBST [10 mM Tris-HCl (pH 7.4)/150 mM NaCl/0.05% (v/v) Tween 20] for dilution of extracts and for washings. Cell extracts were incubated with beads of protein A saturated with: (i) rabbit antibody against  $\beta$ III-tubulin, (ii) mouse monoclonal antibody TuJ1 (IgG2a) against  $\beta$ III-tubulin, (iii) negative control rabbit antibody against non-muscle myosin and (iv) negative control mouse antibody NF-09 or with (v) Immobilized Protein A Plus (Rockford, Illinois, USA) alone. Sedimented beads ( $30\ \mu\text{l}$ ) were incubated for 2 h at  $4^{\circ}\text{C}$  under constant shaking with 0.5 ml of the corresponding antibody in TBST. Antibodies against  $\beta$ III-tubulin (TuJ1) and myosin were used at immunoglobulin concentration 7 and  $4\ \mu\text{g/ml}$ , respectively. Polyclonal affinity purified antibody against  $\beta$ III-tubulin was used at dilution 1:50 and control antibody NF-09 was prepared by mixing 0.4 ml of  $10\times$  concentrated supernatant with 0.8 ml of the TBST buffer. The beads were pelleted by centrifugation at  $5000g$  for 1 min, washed four times (5 min each) in cold TBST, and incubated under rocking overnight at  $4^{\circ}\text{C}$  with 0.5 ml of cell extract, prepared by diluting the extract 1:1 with TBST. The beads were pelleted and washed four times (5 min each) in

cold TBST, followed by boiling for 5 min in 70  $\mu$ l of SDS/sample buffer to release the bound proteins.

### Gel electrophoresis and immunoblotting

SDS/7.5% polyacrylamide gel electrophoresis, electrophoretic transfer of separated proteins onto nitrocellulose and details of the immunostaining procedure are described elsewhere [33]. The anti- $\gamma$ -tubulin monoclonal antibody GTU-88 was diluted 1:5,000, anti- $\beta$ III-tubulin antibody TuJ1 was diluted 1:1,000 and polyclonal anti- $\beta$ III-tubulin antibody was diluted 1:1,000. Bound antibodies were detected after incubation of the blots with secondary anti-mouse or anti-rabbit antibodies conjugated with horseradish peroxidase (dilution 1:10,000), and after washing with SuperSignal WestPico chemiluminescence reagents in accordance with the manufacturer's directions (Pierce, Rockford, Illinois, USA). Exposed autoradiography films X-Omat AR (Eastman Kodak, Rochester, New York, USA) were evaluated using gel documentation system GDS 7500 and GelBase/GelBlot Pro analysis software (UVP, Upland, California, USA).

## Results

### Immunoreactivity profiles of $\beta$ III-tubulin and $\gamma$ -tubulin on primary brain tumors

A description of the cellular distribution of  $\beta$ III-tubulin and  $\gamma$ -tubulin in astrocytic gliomas in accordance with histological type and grade is detailed in our previous publications [5, 17]. Our findings with regard to the present series of tumor samples are consistent with those described in the aforementioned studies [5, 17]. In the 12 astrocytic glioma samples from adult patients, varying degrees of  $\beta$ III-tubulin and  $\gamma$ -tubulin labeling were detected in all histological grades (grades II–IV). However, staining was significantly increased with respect to both proteins in the high-grade anaplastic astrocytomas and glioblastomas multiforme (grades III/IV) ( $\beta$ III-tubulin MLI: 36.7%; IQR: 29.9%–43.5%;  $\gamma$ -tubulin MLI: 43.7%; IQR: 29.3%–57.5%) as compared to the low-grade diffuse astrocytomas (grade II) ( $\beta$ III-tubulin MLI: 4.1%; IQR: 1.4%–8.4%;  $\gamma$ -tubulin MLI: 4.7%; IQR: 3.9%–7.8%) ( $P < 0.05$ ). A similar trend was noted in pediatric tumors but the sample of cases was too small for statistical analysis.

Morphologically, in high-grade astrocytomas, widespread and variably intense  $\beta$ III-tubulin staining was present in the perikaryal cytoplasm and cell processes of astroglial phenotypes (Fig. 1A, C and E). Staining for  $\beta$ III-tubulin in low-grade diffuse astrocytomas was significantly

less widespread but was characterized by considerable heterogeneity of labeling indices among different tumor samples. Intratumoral  $\beta$ III-tubulin staining heterogeneity was noted in individual surgical specimens from both high- and low-grade tumors but was more prevalent in the latter group as previously described [5].

Immunoreactivity for  $\gamma$ -tubulin was characterized by overlapping multipunctate and diffuse staining patterns, which typically merged imperceptibly within individual tumor cells (Fig. 1B, D and F). The cellular distribution of  $\gamma$ -tubulin mirrored that of  $\beta$ III-tubulin in immediately adjacent sections (Fig. 1A–F) insofar as it was more prominent and widespread in high-grade as compared to low-grade tumors.

In normal CNS tissues from patients of different ages,  $\beta$ III-tubulin localization was predominantly neuronal consistent with previous reports [1, 2, 23, 24]. It was absent in glial and mesenchymal cells but was detected in immature neuroepithelial precursor-like cells in the subventricular zone of the telencephalic germinal matrix as previously described [34] (data not shown). In non-neoplastic glia,  $\gamma$ -tubulin labeling was detected in the form of one or two discrete paranuclear dots corresponding to the expected pericentriolar localization of centrosomes as previously described [17].

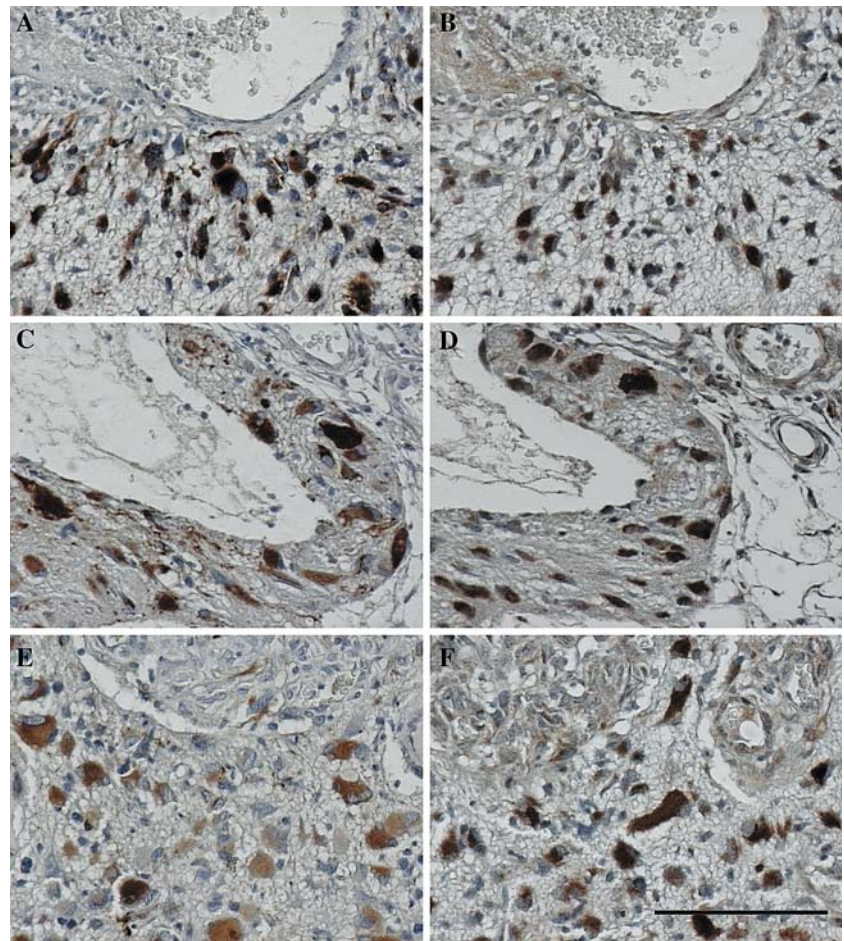
### Co-localization of $\beta$ III-tubulin and $\gamma$ -tubulin in primary tumors

In primary, surgically-resected, astrocytic tumors of all histological grades, co-localization of  $\beta$ III-tubulin and  $\gamma$ -tubulin was demonstrable by confocal microscopy throughout the 'perikaryal' (perinuclear) cytoplasm of tumor cells from low-grade diffuse astrocytomas (Fig. 2A, D and G) and glioblastomas multiforme (Fig. 2B, C, E, F, H and I). In contrast, divergent staining patterns were encountered with respect to glial cell processes where  $\beta$ III-tubulin staining was generally widespread (Fig. 2E, F, H and I) whereas  $\gamma$ -tubulin staining was either absent or present only to a limited degree (Fig. 2B, C, H and I). In keeping with our previous reports [5, 17], the distribution of immunoreactivity for both  $\beta$ III-tubulin and  $\gamma$ -tubulin was more widespread in high-grade as compared to low-grade tumors.

### Differential distribution of $\beta$ III-tubulin and $\gamma$ -tubulin in T98G cells

In T98G glioblastoma cells two distinct patterns of localization were demonstrated using various antibodies to  $\beta$ III-tubulin and  $\gamma$ -tubulin. In Triton X-100 extracted cells, anti- $\beta$ III-tubulin antibodies stained predominantly microtubule arrays and juxta-nuclear cytoplasmic regions (Fig. 3A). In

**Fig. 1** Immunohistochemical localization of  $\beta$ III-tubulin and  $\gamma$ -tubulin in immediately adjacent sections of a glioblastoma multiforme (WHO grade IV). Side-by-side juxtaposition of three representative fields stained with antibodies to  $\beta$ III-tubulin (A, C, E) and  $\gamma$ -tubulin (B, D, F). Avidin-biotin complex peroxidase with hematoxylin counterstain. Scale bar 250  $\mu$ m



contrast no staining was observed in mouse embryonic fibroblast 3T3 cells that were used as negative control (not shown). T98G glioblastoma cells exhibited diffuse and finely granular/confluent micropunctate  $\gamma$ -tubulin staining, that is, in addition to the pericentriolar and juxta-nuclear cytoplasmic localizations (Fig. 3B). These areas of non-MTOC staining were variably robust and were distributed throughout the cytoplasm of T98G cells including the cell's periphery (Fig. 3B and C). Overlapping of  $\beta$ III-tubulin and  $\gamma$ -tubulin labeling was consistently identified in the perinuclear cytoplasmic region known for its microtubule nucleating activity (Fig. 3A and B, arrows, and C). In 3T3 cells, anti- $\gamma$ -tubulin antibodies stained predominantly MTOCs in the perinuclear region as demonstrated previously [28].

We have performed immunofluorescence staining of  $\beta$ III-tubulin and  $\gamma$ -tubulin also in drug-treated T98G cells (taxol, vinblastine and nocodazole) to determine the sub-cellular sorting of these proteins with emphasis on their presence or absence in insoluble aggregates after microtubule disruption. Treatment of cells with taxol caused the formation of microtubule bundles exhibiting marked  $\beta$ III-tubulin staining (Fig. 4A) and incorporation of  $\gamma$ -tubulin in

confluent, variably sized punctate/granular aggregates distributed throughout the cytoplasm (including the peripheral portions) of glioblastoma cells (Fig. 4B). In contrast, treatment with vinblastine caused accumulation of  $\beta$ III-tubulin into tubulin paracrystals (Fig. 4C) while diffuse staining of  $\gamma$ -tubulin was unchanged (Fig. 4D). Exposure of glioblastoma cells to the microtubule depolymerizing drug nocodazole effectively extinguished  $\beta$ III-tubulin staining concomitant with depolymerization of microtubules (Fig. 4E). Unlike  $\gamma$ -tubulin, which retained its multipunctate and/or diffuse staining (Fig. 4F),  $\beta$ III-tubulin was not found in insoluble aggregates following nocodazole treatment (Fig. 4E) (also, see Table 1).

#### $\beta$ III-Tubulin forms complexes with $\gamma$ -tubulin in T98G glioblastoma cells

Extraction of T98G cells with 0.2% Triton X-100 in microtubule stabilizing buffer at 37°C for 1 min, showed that substantial amounts of  $\gamma$ -tubulin and  $\beta$ III-tubulin were present both in soluble and insoluble detergent-resistant pools. There were, however, differences in relative distribution of the proteins under study, after

**Fig. 2** Immunofluorescence localization of  $\gamma$ -tubulin (A–C green) and  $\beta$ III-tubulin (D–F red) in tumor cells from cases of diffuse astrocytoma (grade II) (panels A, D, G) and glioblastoma multiforme (grade IV) (panels B, C, E, F, H and I), Panels A–C (green) and D–F (red) show, respectively, localization of  $\gamma$ -tubulin and  $\beta$ III-tubulin in tumor cells. Superimposition of images in the tumor cell from the grade II astrocytoma demonstrates co-localization (G, yellow). Superimposition of images from the case of glioblastoma multiforme) reveals co-localization of  $\gamma$ -tubulin and  $\beta$ III-tubulin in the perikaryal cytoplasm of tumor cells but lack of  $\gamma$ -tubulin staining in tumor cell fibrillary processes (panels H and I). Laser scanning confocal microscopy performed on paraffin sections. Scale bars (A, D, G) 11  $\mu$ m (B, E, H) 19  $\mu$ m, (C, F, I) 13  $\mu$ m

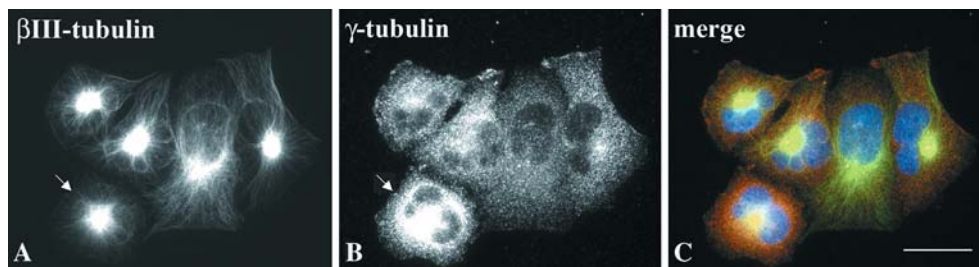
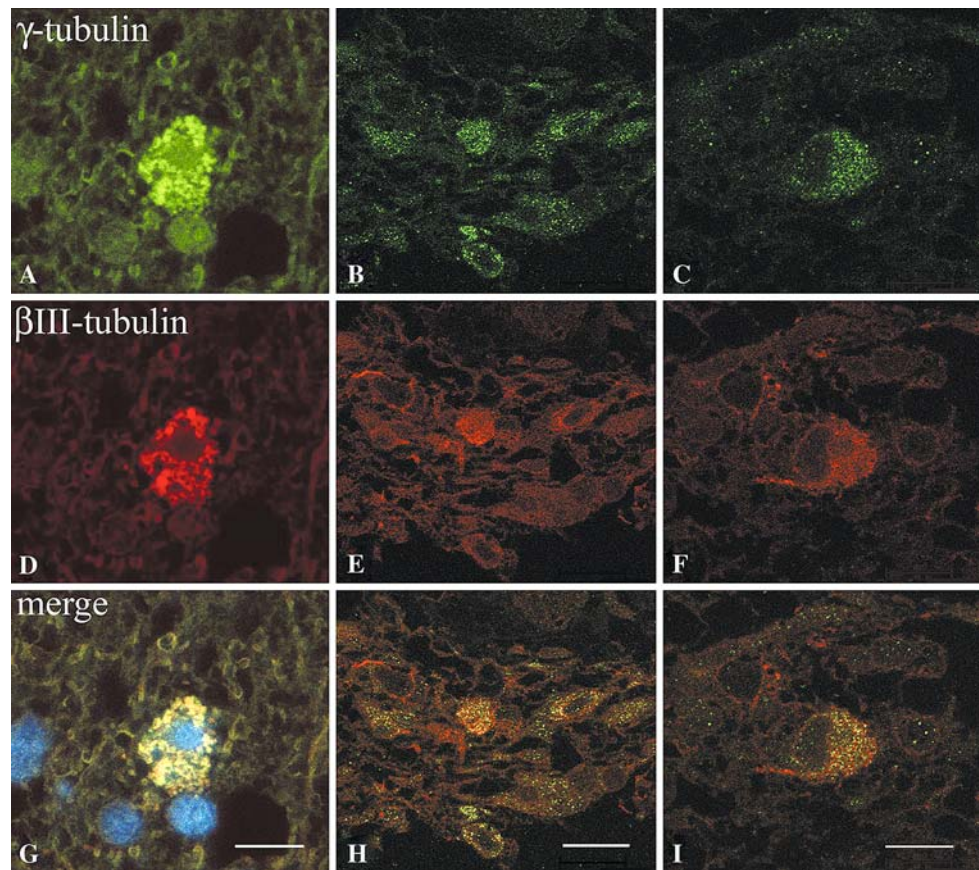


**Fig. 3** Co-expression but differential intracellular distribution of  $\beta$ III-tubulin and  $\gamma$ -tubulin in T98G glioblastoma cells demonstrated by immunofluorescence microscopy. Cells were stained by double labeling with a polyclonal antibody against  $\beta$ III-tubulin (A) and a monoclonal antibody against  $\gamma$ -tubulin (B).  $\beta$ III-Tubulin staining is associated with microtubules (A) whereas  $\gamma$ -tubulin exhibits a

prominent diffuse cytoplasmic localization beyond the pericentriolar region (B). Panel C is an overlay of  $\beta$ III-tubulin (green) and  $\gamma$ -tubulin (red) stainings. Note some overlapping of  $\beta$ III-tubulin and  $\gamma$ -tubulin in perinuclear cytoplasmic region known for its microtubule nucleating activity (A, B arrows) and in the merge image where it is depicted as yellow (C). Scale bar 30  $\mu$ m

disruption of microtubules. The results of a typical same volume experiment are shown in Fig. 5.  $\gamma$ -Tubulin was present in soluble and cytoskeletal fractions in similar quantities both in resting cells and in cells preincubated with nocodazole that efficiently disrupted microtubule arrays, as also confirmed by immunofluorescence microscopy (Fig. 4E). On the other hand,  $\beta$ III-tubulin was present in both soluble and cytoskeletal fractions, in similar quantities, only in untreated cells. When microtubules were depolymerized by nocodazole treatment, a

substantially lower amount of  $\beta$ III-tubulin was detected in the insoluble fraction. These data indicate that the insoluble fraction of  $\gamma$ -tubulin is resistant to nocodazole treatment, while the majority of  $\beta$ III-tubulin can be extracted after nocodazole treatment.

In order to determine whether or not  $\beta$ III-tubulin forms complexes with  $\gamma$ -tubulin, immunoprecipitation experiments with anti- $\beta$ III-tubulin antibodies were performed on extracts from T98G cells. Immunoprecipitation experiments with polyclonal affinity-purified anti- $\beta$ III-tubulin

**Fig. 4** Differential localizations of  $\beta$ III-tubulin (A, C, E) and  $\gamma$ -tubulin (B, D, F) in T98G human glioblastoma cells treated with taxol (A, B), vinblastine (C, D) and nocodazole (E, F). Taxol treatment causes the formation of microtubule bundles showing marked  $\beta$ III-tubulin staining (A) while treatment with vinblastine causes accumulation of  $\beta$ III-tubulin into tubulin paracrystals (C). Nocodazole treatment produces microtubule depolymerization and marked loss of  $\beta$ III-tubulin staining (E). In contrast,  $\gamma$ -tubulin retains its multipunctate and/or diffuse staining after treatment with used drugs (B, D, F). Scale bar 30  $\mu$ m

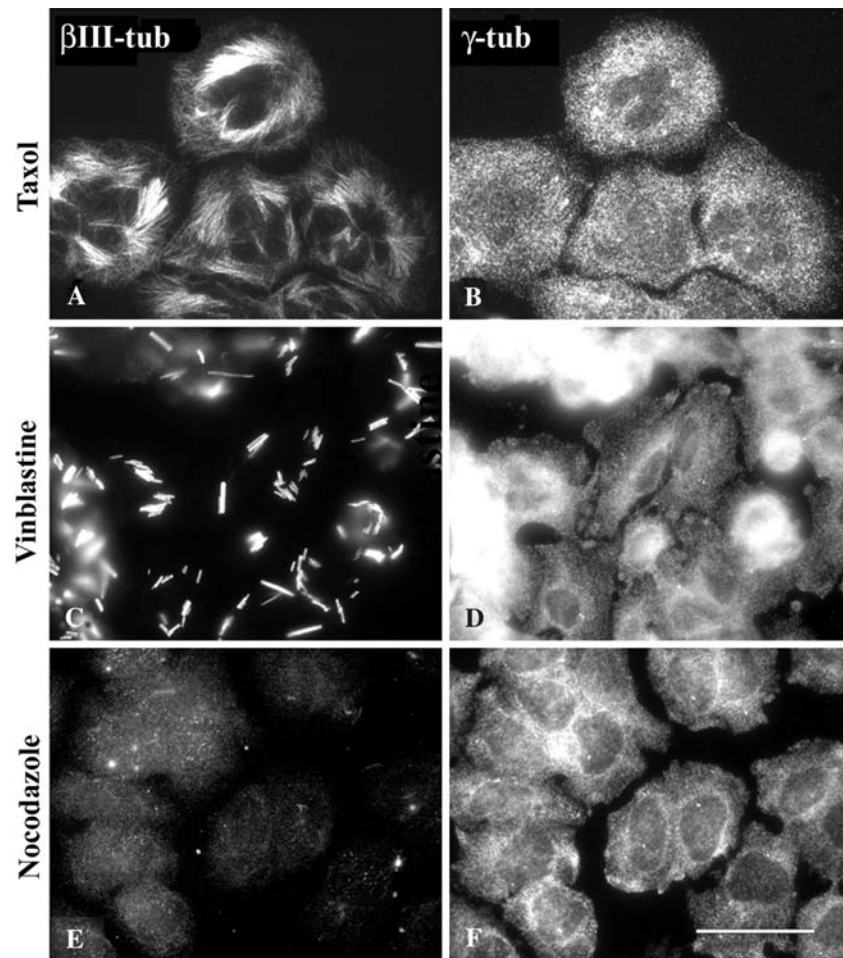


**Table 1** Immunofluorescent staining patterns of  $\beta$ III-tubulin and  $\gamma$ -tubulin in T98G human glioblastoma cells after nocodazole treatment

Antigen	Basal conditions	Nocodazole treatment	Comment
$\beta$ III-Tubulin	+++ MT arrays	Abolition of MT staining	Depolymerization effect
$\gamma$ -Tubulin	++/+++ Diffuse cytoplasmic/micropunctate	++/+++ Diffuse cytoplasmic/micropunctate	Insoluble aggregates

Abbreviation: MT, microtubule

Scale of reactivity: ++ moderate, +++ prominent/robust

antibody immobilized on protein A showed co-precipitation of  $\gamma$ -tubulin (Fig. 6A, panel “ $\gamma$ -Tb”, lane 2). The similar staining was observed with monoclonal antibodies GTU-88 and TU-32 directed against a different epitopes on  $\gamma$ -tubulin molecule. No staining in  $\gamma$ -tubulin region was observed when immobilized antibody was incubated without the extract (Fig. 6A, panel “ $\gamma$ -Tb”, lane 3) or when protein A without the antibody was incubated with extracts (Fig. 6A, panel “ $\gamma$ -Tb”, lane 4). When the negative control antibody against myosin was used for immunoprecipitation, no  $\gamma$ -tubulin was detected (not shown). When immunoprecipitated proteins were probed with monoclonal antibody TuJ1 against  $\beta$ III-tubulin,

distinct  $\beta$ -tubulin was detected (Fig. 6A, panel “ $\beta$ III-Tb”, lanes 2). A similar set of immunoprecipitation experiments was performed with monoclonal antibody TuJ1 used for immunoprecipitation. Precipitated  $\gamma$ -tubulin was detected by anti- $\gamma$ -tubulin antibody GTU-88 and precipitated  $\beta$ III-tubulin with polyclonal antibody against  $\beta$ III-tubulin (Fig. 6B). As negative control for precipitation served in this case monoclonal antibody NF-09 against neurofilament protein NF-M. In this precipitation arrangement,  $\gamma$ -tubulin was also specifically co-precipitated with anti- $\beta$ III-tubulin antibody. Soluble  $\beta$ III-tubulin, therefore, forms complexes with  $\gamma$ -tubulin in T98G human glioblastoma cells.

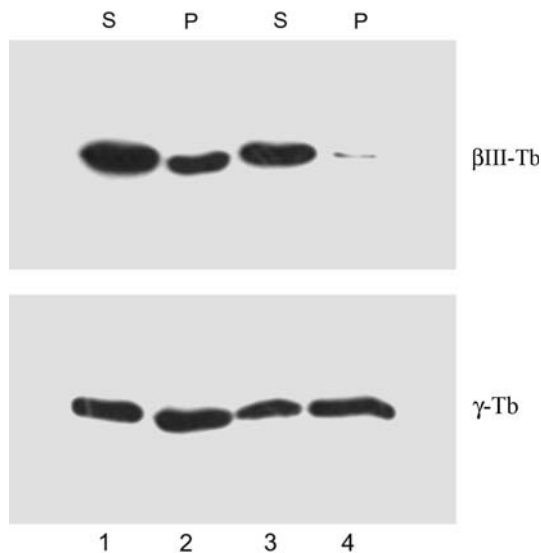


**Fig. 5** Immunoblot analysis of soluble and insoluble fractions from human glioblastoma cell line T98G. Samples were prepared from untreated cells (lanes 1 and 2) or from cells pre-treated with nocodazole to disrupt microtubule arrays (lanes 3 and 4). To compare the relative distribution of immunoblotted proteins, pelleted material was resuspended in a volume equal to the corresponding supernatant. Immunostaining with antibody TuJ1 against  $\beta$ III-tubulin ( $\beta$ III-Tb) and antibody TU-32 against  $\gamma$ -tubulin ( $\gamma$ -Tb). S, supernatant; P, pellet

## Discussion

Differential subcellular sorting of  $\gamma$ -tubulin and  $\beta$ III-tubulin in glioblastoma cells

Diploid cells, including non-transformed human astrocytes contain one or two juxtannuclear centrosomes typified by

pericentriolar staining for  $\gamma$ -tubulin [17]. Although T98G glioblastoma cells recapitulate -in part- this pericentriolar pattern of distribution, they also exhibit highly prominent diffuse cytoplasmic  $\gamma$ -tubulin staining indicating that under neoplastic conditions this centrosome-associated protein is either incorporated into insoluble (oligomeric) aggregates, associated with membraneous components, or is part of an increased soluble pool distributed throughout the cytoplasm of tumor cells. In contrast,  $\beta$ III-tubulin, co-expressed in glioblastoma cells, exhibited a predominantly cytoskeletal distribution associated with cytoplasmic microtubule arrays.

The subcellular sorting of these two proteins in glioblastoma cells was further elucidated following treatment of T98G cells with microtubule-acting drugs. Exposure to taxol led to the formation of  $\beta$ III-tubulin labeled microtubule bundles while prominent micropunctate and diffuse  $\gamma$ -tubulin staining was unchanged. Previous studies have shown that expression  $\beta$ III-tubulin in non-neuronal tumors is associated with resistance to taxanes [35–40]. However, the effect of taxol on  $\beta$ III-tubulin enriched microtubules in glioma cells is -to our knowledge- unknown and warrants further elucidation. Vinblastine treatment of glioblastoma cells led to the incorporation of  $\beta$ III-tubulin into tubulin paracrystals, while  $\gamma$ -tubulin distribution was not effected. In contrast, treatment with nocodazole, a microtubule-depolymerizing agent, led to microtubule disruption and marked diminution of  $\beta$ III-tubulin staining. Thus,  $\beta$ III-tubulin in T98G glioblastoma is not associated with insoluble cytoplasmic aggregates of  $\gamma$ -tubulin.

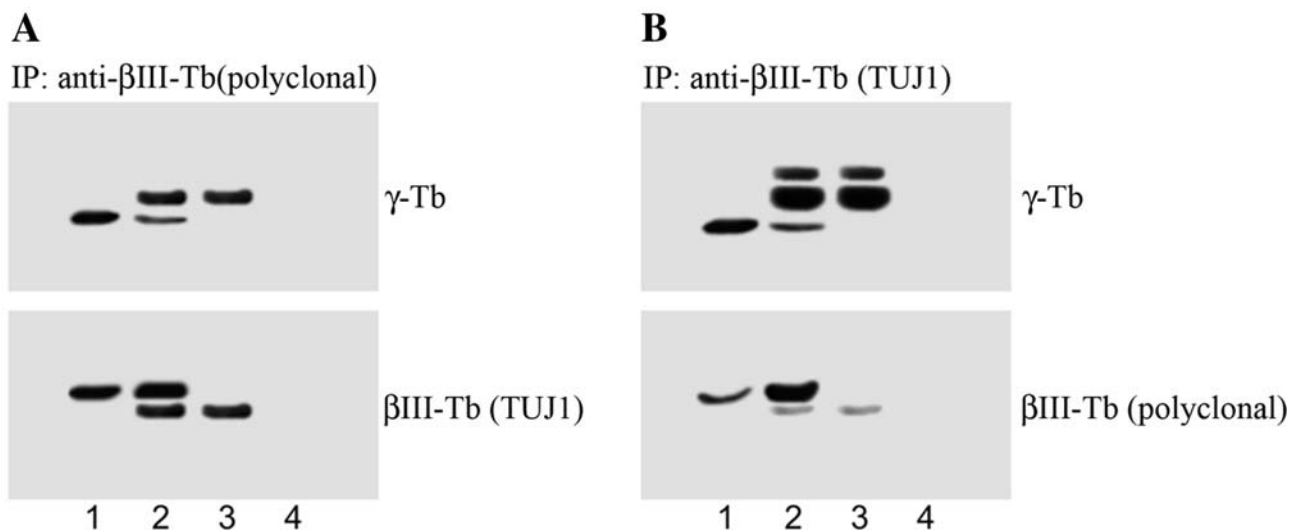


**Fig. 6** Immunoprecipitation of extract from glioblastoma cell line T98G with polyclonal (A) and monoclonal TuJ1 (B) anti- $\beta$ III-tubulin antibodies. Samples were precipitated with anti- $\beta$ III-tubulin antibodies immobilized to protein A. Blots were probed with monoclonal antibody GTU-88 against  $\gamma$ -tubulin ( $\gamma$ -Tb), monoclonal antibody TuJ1 against  $\beta$ III-tubulin (TUJ1) and polyclonal anti-  $\beta$ III-tubulin antibody

(polyclonal). Cell extract after precipitation (lane 1), immunoprecipitated proteins (lane 2), immobilized immunoglobulin not incubated with cell extract (lane 3), proteins from cell extract bound to carrier without antibody (lane 4) NOTE: For interpretation of the references to color in this figure legend, the reader is referred to the online version of this article

## Interaction of $\beta$ III-tubulin and $\gamma$ -tubulin in glioblastoma cells

Aside from the co-expression and differential compartmentalization of  $\beta$ III-tubulin and  $\gamma$ -tubulin in the human glioblastoma cell line T98G the present study has also demonstrated for the first time evidence of interaction between  $\beta$ III-tubulin and  $\gamma$ -tubulin in animal cells in general and human glioblastoma cells in particular. It is well established that in cells the majority of  $\gamma$ -tubulin is associated with other proteins in soluble cytoplasmic complexes. The so-called large  $\gamma$ -tubulin-ring complex ( $\gamma$ -TuRC) [11, 41] is formed by small complexes ( $\gamma$ -tubulin small complex;  $\gamma$ -TuSC) [42], comprising two molecules of  $\gamma$ -tubulin, one molecule each of  $\gamma$ -tubulin complex protein 2 (GCP2) and GCP3 [43] and some other proteins. However, there are reports indicating that variable amounts of tubulin dimers are capable of co-precipitating with  $\gamma$ -tubulin in preparations from *Xenopus* oocytes [11], chicken erythrocytes [44], porcine brain [16], ovine brain [45] and from plants [46]. However, it is not known at the present time, if there are any differences of interaction of  $\gamma$ -tubulin with tubulin dimers as regards  $\alpha/\beta$ -tubulin dimer isotypes.

### $\beta$ III-Tubulin and $\gamma$ -tubulin in glioma tumorigenesis

Neoplastic cells, particularly the highly malignant or anaplastic tumor phenotypes, may exhibit aberrant microtubule nucleation through centrosome abnormalities resulting in modified functional properties of microtubules. It is possible that in the course of malignant transformation of glioma cells such altered or ectopic MTOCs could be accompanied by changes in tubulin synthesis and tubulin isotype composition of microtubules potentially associated with abnormalities involving tumor cell architecture, polarity, adhesion and motility, including the capacity to invade and infiltrate host brain tissues.

Alterations in the expression and post-translational modification of tubulin isotypes may have particular relevance in tumorigenesis and tumor progression [1, 2]. Upregulation of certain tubulin forms may represent molecular features associated with anaplastic change in gliomas. To this end, screening of multiple molecules with oligonucleotide microarray analysis has shown that  $\beta$ IV- and  $\gamma$ -tubulins are upregulated in high- versus low-grade gliomas [47]. The findings of the present study, notably that  $\beta$ III-tubulin and  $\gamma$ -tubulin are co-distributed in tumor cells of primary astroglial tumors and furthermore that these two proteins co-precipitate in soluble fractions of cultured glioblastoma cells, lend credence to the notion of an altered interaction of  $\beta$ III-tubulin with enhanced levels of  $\gamma$ -tubulin in the context of cancer-associated centrosome amplification [17]. This assertion is further supported by the

existing knowledge that  $\gamma$ -tubulin interacts with  $\alpha/\beta$ -tubulin dimers [16].

Previous studies have shown that class III  $\beta$ -tubulin is expressed in human glioblastoma cell line U251MG [48] and in glioma-derived clones in vitro either in the form of cells which lack GFAP staining, as well as in single cells co-expressing both  $\beta$ III-tubulin and GFAP [49]. The U251MG line is derived from a glioblastoma with p53 mutant status, like the T98G line [18]. It is known that deletion or mutational/functional inactivation of p53 leads to centrosome dysfunction including centrosome amplification [50]. Because *TP53* gene mutations are genotypic hallmarks of ‘secondary’ glioblastomas, which arise as a consequence of malignant change in pre-existing diffuse low-grade astrocytomas [51], it is possible that mutational inactivation of p53 may potentially result in centrosome amplification and abnormal cellular distribution of  $\gamma$ -tubulin in the p53-mutant T98G human glioblastoma line. However, as we have recently shown, ectopic patterns of  $\gamma$ -tubulin distribution were present both in human glioblastoma cell lines expressing either mutant p53 (T98G, U118MG and U138MG) or wild-type p53 (U87MG) [17]. It remains to be determined whether there are differences of  $\gamma$ -tubulin mRNA expression in p53-wild type versus p53-mutant glioblastoma cell lines and whether these relate to  $\beta$ III-tubulin expression.

In summary, our results show for the first time that  $\beta$ III-tubulin in neoplastic astrocytes is accompanied by highly prominent ectopic  $\gamma$ -tubulin distribution. Interactions of both tubulins were observed in soluble cytoplasmic pools from T98G human glioblastoma cells. However, the nature of this interaction remains to be determined in future functional studies focusing on its relation to the cell cycle as well as the expression and post-translational modifications of the full repertoire of tubulin isotypes. We suggest that aberrant expression and interactions of  $\beta$ III-tubulin and  $\gamma$ -tubulin may be linked to malignant changes in glial cells.

**Acknowledgments** We thank Dr. Jennian F. Geddes, Department of Histopathology and Morbid Anatomy, Queen Mary, University of London, The Royal London Hospital, London, England and Dr. Theodoros Maraziotis, Department of Neurosurgery, University Hospital, Patras, Greece for the procurement of archival tissue material from brain tumor cases. We thank Dr. Anthony Frankfurter, Department of Biology, University of Virginia, Charlottesville, for his gift of monoclonal antibody TuJ1 and the polyclonal antibody to  $\beta$ III-tubulin. Supported by an Established Investigator Award from the St. Christopher’s Foundation for Children (to C.D. Katsetos), LC545 from the Ministry of Education of the Czech Republic, and by Institutional Research Support AVOZ 50520514 (to P. Dráber).

## References

1. Katsetos CD, Herman MM, Mörk SJ (2003) Class III  $\beta$ -tubulin in human development and cancer. *Cell Motil Cytoskeleton* 55:77–96

2. Katsetos CD, Legido A, Perentes E et al (2003) Class III  $\beta$ -tubulin isotype: a key cytoskeletal protein at the crossroads of developmental neurobiology and tumor neuropathology. *J Child Neurol* 18:851–866
3. Dráberová E, Lukáš A, Ivanyi D et al (1998) Expression of class III  $\beta$ -tubulin in normal and neoplastic human tissues. *Histochem Cell Biol* 109:231–239
4. Katsetos CD, Del Valle L, Legido A et al (2003) On the neuronal/neuroblastic nature of medulloblastomas: a tribute to Pio del Rio Hortega and Moises Polak. *Acta Neuropathol (Berl)* 105:1–13
5. Katsetos CD, Del Valle L, Geddes JF et al. (2001) Aberrant localization of the neuronal class III  $\beta$ -tubulin in astrocytomas: a marker for anaplastic potential. *Arch Pathol Lab Med* 125:613–624
6. Martinez-Diaz H, Kleinschmidt-DeMasters BK, Powell SZ et al (2003) Giant cell glioblastoma and pleomorphic xanthoastrocytoma show different immunohistochemical profiles for neuronal antigens and p53 but share reactivity for class III  $\beta$ -tubulin. *Arch Pathol Lab Med* 127:1187–1191
7. Katsetos CD, Del Valle L, Geddes JF et al (2002) Localization of the neuronal class III  $\beta$ -tubulin in oligodendrogliomas: Comparison with Ki-67 proliferative index and 1p/19q status. *J Neuropathol Exp Neurol* 61:307–320
8. Giannini C, Scheithauer BW, Lopes MB et al (2002) Immunophenotype of pleomorphic xanthoastrocytoma. *Am J Surg Pathol* 26:479–485
9. Aldaz H, Rice LM, Stearns T et al (2005) Insights into microtubule nucleation from the crystal structure of human  $\gamma$ -tubulin. *Nature* 435:523–527
10. Joshi HC, Palacios MJ, McNamara L et al (1992)  $\gamma$ -Tubulin is a centrosomal protein required for cell cycle-dependent nucleation. *Nature* 356:80–82
11. Zheng Y, Wong ML, Alberts B et al (1995) Nucleation of microtubule assembly by  $\gamma$ -tubulin-containing ring complex. *Nature* 378:578–583
12. Zhou J, Shu H-B, Joshi HC (2002) Regulation of tubulin synthesis and cell cycle progression in mammalian cells by  $\gamma$ -tubulin-mediated microtubule nucleation. *J Cell Biochem* 84:472–483
13. Inclan YF, Nogales E (2001) Structural models for the self-assembly and microtubule interactions of  $\gamma$ -,  $\delta$ - and  $\epsilon$ -tubulin. *J Cell Sci* 114:413–422
14. Llanos R, Chevrier V, Ronjat M et al (1999) Tubulin binding sites on  $\gamma$ -tubulin: identification and molecular characterization. *Biochemistry* 38:15712–15720
15. Paluh JL, Nogales E, Oakley BR et al (2000) A mutation in  $\gamma$ -tubulin alters microtubule dynamics and organization and is synthetically lethal with the kinesin like protein Pkl1p. *Mol Biol Cell* 11:1225–1239
16. Sulimenko V, Sulimenko T, Poznanovic S et al (2002) Association of brain  $\gamma$ - tubulins with  $\alpha\beta$ -tubulin dimers. *Biochem J* 365:889–895
17. Katsetos CD, Reddy G, Dráberová E et al (2006) Altered cellular distribution and subcellular sorting of  $\gamma$ -tubulin in astrocytic gliomas and human glioblastoma cell lines. *J Neuropathol Exp Neurol* 65:465–477
18. Stein GH (1979) T98G: an anchorage-independent human tumor cell line that exhibits stationary phase G1 arrest in vitro. *J Cell Physiol* 99:43–54
19. Ito H, Kanzawa T, Kondo S et al (2005) Microtubule inhibitor D-24851 induces p53- independent apoptotic cell death in malignant glioma cells through Bcl2 phosphorylation and Bax translocation. *Int J Oncol* 26:589–596
20. Alexander JE, Hunt DF, Shabanowitz J et al (1991) Characterization of posttranslational modifications in neuron specific class III  $\beta$ -tubulin by mass spectrometry. *Proc Natl Acad Sci (USA)* 88:4685–89
21. Lee MK, Tuttle JB, Rebhun LI et al (1990) The expression and posttranslational modification of a neuron-specific  $\beta$ -tubulin isotype during chick embryogenesis. *Cell Motil Cytoskeleton* 17:118–132
22. Lee MK, Rebhun LI, Frankfurter A (1990) Posttranslational modification of class III  $\beta$ -tubulin. *Proc Natl Acad Sci USA* 87:7195–7199
23. Katsetos CD, Frankfurter A, Christakos S et al (1993) Differential localization of class III  $\beta$ -tubulin isotype and calbindin-D28k defines distinct neuronal types in the developing human cerebellar cortex. *J Neuropathol Exp Neurol* 52:655–666
24. Katsetos CD, Karkavelas G, Herman MM et al (1998) Class III  $\beta$ -tubulin isotype ( $\beta$ III) in the adrenal medulla: I. Localization in the developing human adrenal medulla. *Anat Rec* 250:335–343
25. Ziková M, Sulimenko V, Dráber P et al (2000) Accumulation of 210 kDa microtubule-interacting protein in differentiating P19 embryonal carcinoma cells. *FEBS Lett* 473:19–23
26. Kukharskyy V, Sulimenko V, Macůrek L et al (2004) Complexes of  $\gamma$ -tubulin with non-receptor protein tyrosin kinases Src and Fyn in differentiating P19 embryonal carcinoma cells. *Exp Cell Res* 298:218–228
27. Katsetos CD, Kontogeorgos G, Geddes JF et al (2000) Differential distribution of the neuron-associated class III  $\beta$ -tubulin in neuroendocrine lung tumors. *Arch Pathol Lab Med* 124:535–544
28. Nováková M, Dráberová E, Schürmann W et al (1996)  $\gamma$ -Tubulin redistribution in taxol-treated mitotic cells probed by monoclonal antibodies. *Cell Motil Cytoskeleton* 33:38–51
29. Libusová L, Sulimenko T, Sulimenko V et al. (2004)  $\gamma$ -Tubulin in Leishmania: cell- cycle dependent changes in subcellular localization and heterogeneity of its isoforms. *Exp Cell Res* 295:375–386
30. Sulimenko V, Dráberová E, Sulimenko T et al (2006) Regulation of microtubule formation in activated mast cells by complexes of  $\gamma$ -tubulin with Fyn and Syk kinases. *J Immunol* 176:7243–7253
31. Dráberová E, Sulimenko V, Kukharskyy V et al (1999) Monoclonal antibody NF-09 specific for neurofilament protein NF-M. *Fol Biol. Praha* 45:163–165
32. Dráberová E, Dráber P (1993) A microtubule-interacting protein involved in coalignment of vimentin intermediate filaments with microtubules. *J Cell Sci* 106:1263–1273
33. Dráber P, Lagunowich LA, Dráberová E et al (1988) Heterogeneity of tubulin epitopes in mouse fetal tissues. *Histochemistry* 89:485–492
34. Weickert CS, Webster MJ, Colvin SM et al (2000) Localization of epidermal growth factor receptors and putative neuroblasts in human subependymal zone. *J Comp Neurol* 423:359–372
35. Dumontet C, Isaac S, Souquet PJ et al (2005) Expression of class III  $\beta$ -tubulin in non-small cell lung cancer is correlated with resistance to taxane chemotherapy. *Bull Cancer* 92:E25–30
36. Kamath K, Wilson L, Cabral F et al (2005)  $\beta$ III-tubulin induces paclitaxel resistance in association with reduced effects on microtubule dynamic instability. *J Biol Chem* 280:12902–12907
37. Kavallaris M, Kuo DYS, Burkhart CA et al (1997) Taxol-resistant epithelial ovarian tumors are associated with altered expression of specific  $\beta$ -tubulin isoforms. *J Clin Invest* 100:1282–1293
38. Mozzetti S, Ferlini C, Concolino P et al. (2005) Class III  $\beta$ -tubulin overexpression is a prominent mechanism of paclitaxel resistance in ovarian cancer patients. *Clin Cancer Res* 11:298–305
39. Ranganathan S, Benetatos CA, Colarusso PJ et al (1998) Altered  $\beta$ -tubulin isotype expression in paclitaxel-resistant human prostate carcinoma cells. *Br J Cancer* 77:562–566
40. Tommasi S, Mangia A, Lacalamita R et al (in press) Cytoskeleton and paclitaxel sensitivity in breast cancer: the role of  $\beta$ -tubulins. *Int J Cancer*

41. Moritz M, Braunfeld MB, Sedat JW et al (1995) Microtubule nucleation by  $\gamma$ -tubulin-containing rings in the centrosome. *Nature* 378:638–640
42. Moritz M, Zheng Y, Alberts BM et al (1998) Recruitment of the  $\gamma$ -tubulin ring complex to *Drosophila* salt-stripped centrosome scaffolds. *J Cell Biol* 142:775–786
43. Oegema K, Wiese C, Martin OC et al. (1999) Characterization of two related *Drosophila*  $\gamma$ -tubulin complexes that differ in their ability to nucleate microtubules. *J Cell Biol* 144:721–733
44. Linhartová I, Novotná B, Sulimenko V et al (2002)  $\gamma$ -Tubulin in chicken erythrocytes: changes in localization during cell differentiation and characterization of cytoplasmic complexes. *Dev Dynam* 223:229–240
45. Detraves C, Mazarguil H, Lajoie-Mazenc I et al (1997) Protein complexes containing  $\gamma$ -tubulin are present in mammalian brain microtubule protein preparations. *Cell Motil Cytoskeleton* 36:179–189
46. Dryková D, Cenklová V, Sulimenko V et al (2003) Plant  $\gamma$ -tubulin interacts with  $\alpha\beta$ -tubulin dimers and forms membrane-associated complexes. *Plant Cell* 15:465–480
47. Rickman DS, Bobek MP, Misek DE et al (2001) Distinctive molecular profiles of high-grade and low-grade gliomas based on oligonucleotide microarray analysis. *Cancer Res* 61:6885–6891
48. Lopes MB, Frankfurter A, Zientek GM et al (1992) The presence of neuron-associated microtubule proteins in the human U-251 MG cell line. A comparative immunoblot and immunohistochemical study. *Mol Chem Neuropathol* 17:273–287
49. Ignatova TN, Kukekov VG, Laywell ED et al (2002) Human cortical glial tumors contain neural stem-like cells expressing astroglial and neuronal markers in vitro. *Glia* 39:193–206
50. Tarapore P, Fukasawa K (2002) Loss of p53 and centrosome hyperamplification. *Oncogene* 21:6234–6240
51. Ohgaki H, Kleihues P (2005) Population-based studies on incidence, survival rates, and genetic alterations in astrocytic and oligodendroglial gliomas. *J Neuropathol Exp Neurol* 64:479–489